Kinetic Mechanism of a Partial Folding Reaction. 1. Properties of the Reaction and Effects of Denaturants†

Jonathan M. Goldberg and Robert L. Baldwin*

Department of Biochemistry, Beckman Center, Stanford University Medical Center, Stanford, California 94305-5307

Received September 29, 1997; Revised Manuscript Received December 29, 1997

ABSTRACT: The bimolecular association rate constant (k_{on}) and dissociation rate constant (k_{off}) of the complex between fluorescein-labeled S-peptide analogues and *folded* S-protein are reported. This is the first kinetic study of a protein folding reaction in which most of the starting material is already folded and only a small part (one additional helix) becomes ordered; it provides a folding landscape with a small conformational entropy barrier, and one in which kinetic traps are unlikely. Refolding and unfolding are measured under identical strongly native conditions, and the reaction is found to be two-state at low reactant concentrations. The dissociation constant (K_d) of the complex and the properties of the transition state may be calculated from the rate constants without extrapolation. The folded complex is formed fast ($k_{on} = 1.8 \times 10^7$ M^{-1} s^{-1}) and is very stable ($K_d = 6$ pM) at 10 °C, 10 mM MOPS, pH 6.7. Charge interactions stabilize the complex by 1.4 kcal mol^{-1}. The charge effect enters in the refolding reaction: increasing the salt concentration reduces k_{on} dramatically and has little effect on k_{off}. Urea and GdmCl destabilize the complex by decreasing k_{on} and increasing k_{off}. The slopes (*m*-values) of plots of ln K_d vs [cosolvent] are 0.75 ± 0.04 and 2.8 ± 0.3 kcal mol^{-1} M^{-1} for urea and GdmCl, respectively. The ratio $m_{on}/(m_{on} + m_{off})$ is 0.54 ± 0.04 for urea and 0.57 ± 0.1 for GdmCl, where m_{on} is the *m*-value for k_{on} and m_{off} is the *m*-value for k_{off}, indicating that more than half of the sites for interaction with either cosolvent are buried in the ensemble of structures present at the transition state.

The refolding kinetics of numerous small proteins obey simple exponential kinetics, indicating that intermediates are not populated and that these polypeptides cross a free-energy barrier before reaching their native states (for recent examples see refs 1 and 2). This free energy barrier may be the wall of a kinetic trap or a decrease in conformational entropy before the formation of stabilizing protein−protein interactions (*3*, *4*). There may also be an enthalpic barrier in simple refolding reactions (*5*). Both the depth of kinetic traps and the height of the conformational entropy barrier to refolding are expected to decrease dramatically with decreasing chain length, but the shortest stable proteins are of the order of 60 residues. We present data for the reaction

$$p + N \underset{k_{off}}{\overset{k_{on}\,[\text{S-pro}]}{\rightleftharpoons}} pN \qquad (1)$$

where p is a fluorescently labeled S-peptide analogue, N is the *folded* form of S-protein, and pN is the S-peptide analogue/S-protein (RNaseS*[1]) complex. Our aim is to characterize the free energy barrier on a folding landscape which has a low conformational entropy barrier and is unlikely to contain deep kinetic traps. The conformational entropy lost during folding is chiefly that of the 15 residue S-peptide analogue.

Protein folding reactions with exponential time courses may be well described by the transition state theory (*6*). The observed rate constant of such a reaction is the product $K^{\ddagger}k^{\ddagger}$, where $K^{\ddagger}$ is the equilibrium constant for formation of the activated complex ($I^{\ddagger}$) from reactants, and $k^{\ddagger}$ is the rate constant of a subsequent elementary conformational step on the folding landscape (eq 2)

$$A \overset{K^{\ddagger}}{\rightleftharpoons} I^{\ddagger} \overset{k^{\ddagger}}{\longrightarrow} B \qquad (2)$$

where the reaction is reversible and A or B may be either product or reactant, depending on the experimental conditions. The rate constants of protein folding reactions report on the values of $K^{\ddagger}$ and $k^{\ddagger}$. The fluorescent label on S-peptide allows the bimolecular association rate constant for forming RNaseS* to be measured readily in a rapid mixing experiment under strongly native conditions. An important advantage of the RNaseS* system is that the dissociation of labeled S-peptide analogue may be monitored

† This work was supported by a grant from the National Institutes of Health (GM 19988). J.M.G. was supported in part by a postdoctoral fellowship from the American Cancer Society (PF 3803). The Mass Spectrometry Facility at the University of California, San Francisco, was supported by National Institutes of Health Grant RR 01614.

* To whom correspondence should be addressed: phone, (650) 723-6168; fax, (650) 723-6783; e-mail, goldberg@cmgm.stanford.edu.

[1] Abbreviations: ACN, acetonitrile; CD, circular dichroism; 2′3′CMP, 2′3′ cyclic cytodine monophosphate; DIEA, diisopropylethylamine; DMAP, (dimethylamino)pyridine; DMF, dimethylformamide; NH_4Ac, ammonium acetate; Pep-1, Ac−YETAAAKFERQHMDS−NH_2; Pep-1F, Pep-1 labeled via an amide linkage between N^{ϵ} of lysine-7 and the 5-carbonyl carbon of fluorescein; M13A-1, Ac−YETAAAKFERQHADS−NH_2; M13A-1F, M13A-1 labeled as described for Pep-1F; RNaseA, bovine pancreatic ribonuclease A; S-peptide, RNaseA fragment comprised of residues 1−20; S-protein, RNaseA fragment comprised of residues 21−124; S-Pro, S-protein; RNaseS, complex between S-protein and S-peptide; RNaseS*, complex between a fluorescently labeled S-peptide analogue and S-protein; TFE, trifluoroethanol.

S0006-2960(97)02402-1 CCC: $15.00
Published on Web 02/06/1998

under the same conditions as refolding by competition with an excess of the unlabeled analogue. The folding equilibrium constant may thus be calculated directly from the rate constants, and some physical properties of $I^{\ddagger}$ may be inferred from k_{on} and k_{off} without extrapolation. Sauer and co-workers used a similar strategy to characterize the transition barrier of the Arc-repressor dimer (*7*), which involves ordering of a much larger polypeptide chain.

In this article we characterize the reaction between S-peptide analogues and folded S-protein and confirm that the reaction is two-state. The denaturant and salt dependences of the reaction are measured in conjunction with this basic characterization. The solvent accessibility and stabilization of $I^{\ddagger}$ by charge interactions are discussed. In the next article we characterize the effects of S-peptide mutations and temperature on the transition state. We also exploit the advantage of the RNaseS* system that allows measurement of the viscosity dependences of k_{on} and k_{off} under identical strongly native conditions.

MATERIALS AND METHODS

S-Protein. RNase S was prepared from RNase A by cleavage with subtilisin (*8*); S-peptide and S-protein were separated by gel filtration (*9*). The concentration of S-protein was determined by the absorbance at 267 nM in pH 2 100 mM glycine buffer. An extinction coefficient of 7450 cm^{-1} M^{-1} was determined from quantitative amino acid analysis (Protein and Nucleic Acid Facility, Stanford University Medical Center, Stanford, CA). S-protein was stored lyophilized, and stock solutions dissolved in water. S-protein was incubated at the final experimental conditions for at least 1 h before individual experiments.

Peptide Design and Synthesis. The sequences and abbreviations of the two S-peptide analogues characterized in this article are Pep-1, Ac−YETAAAKFERQHMDS−NH_2, and M13A-1, Ac−YETAAAKFERQHADS−NH_2. They are similar to S-peptide (*8*), except residues 16−20 are not included since they are disordered in RNaseS (*10*). The peptide was acetylated, and Lys-1 was replaced with Tyr so that N^{ϵ} of Lys-7 would be the sole reactive site for 5-carboxyfluorescein succinimidyl ester, and to provide a spectroscopic probe for the concentration of unlabeled peptide. Peptides were synthesized and purified as described previously (*11*), stored lyophilized, and dissolved in water before use. Concentrations were determined by the absorbance at 280 nm using an extinction coefficient for tyrosine of 1390 cm^{-1} M^{-1} (*12*).

Peptide Labeling. Peptides were derivatized at Lys-7 with a fluorescein analogue since this provides a sensitive probe for binding to S-protein (*13*). Purified peptides were labeled using a modified protocol from Molecular Probes. Ten milligrams of Pep-1 or M13A-1 was dissolved in 1 mL of water, and 10 mg of 5-carboxyfluorescein succinimidyl ester (Molecular Probes) was dissolved in 1 mL of DMF. The two solutions were added to 8 mL of DMF containing 7.5 μL of DIEA and 400 μg of DMAP and agitated overnight at room temperature in a foil-shielded container.

Purification of Labeled Peptides. The reaction mixture was diluted 10-fold into 0.1% trifluoroacetic acid and loaded onto a Sep-Pak C_{18} cartridge (Millipore) which had been washed with ACN. The peptide was eluted in a minimum volume of 10 mM NH_4Ac, 50% ACN, lyophilized, and redissolved in a minimum volume of 10 mM NH_4Ac, 14% ACN. Labeled analogues were purified in 10 mM NH_4Ac using an ACN gradient on an FPLC system equipped with a PepRPC HR16/10 C_{18} column (Pharmacia). The purified fractions were divided into aliquots, lyophilized, and stored in foil-shielded containers at −20 °C.

Analysis of Labeled Peptides. The compositions of the peptides were verified by mass spectrometry (Mass Spectrometry Facility, University of California, San Francisco), amino acid analysis, and peptide sequencing (Protein and Nucleic Acid Facility, Stanford University Medical Center, Stanford, CA). The concentrations of the S-peptide analogues were determined from the absorbance at 496 nm in 100 mM CHES buffer, pH 9.0, using an extinction coefficient of 76 000 cm^{-1} M^{-1} based on that of free 5-fluorescein succinimidyl ester (Molecular Probes catalog, 1992−1994). The yields of Pep-1F and M13A-1F from Pep-1 and M13A-1 were about 35%. Freshly synthesized Pep-1F, but not M13A-1F, is contaminated by about 5% of an analogue eluting at slightly lower ACN concentration, which is likely to be the peptide containing S^{δ} methionine sulfoxide. The amount of this contaminant does not increase during storage of the lyophilate but does once the analogue is dissolved in water.

Circular Dichroism Measurement. The CD spectrum of Pep-1F was acquired as described previously (*14*). The conditions were 20 μM Pep-1F, 1 mM potassium phosphate, pH 7.25, 10 mM potassium fluoride, and 0 °C. The fraction helix, *f*, was calculated from, $[\theta]_{222}$, the mean residue ellipticity at 222 nm, in units of deg cm^2 $dmol^{-1}$, using the expression $f = [\theta]_{222}/(\theta_H - \theta_C)$. $\theta_H = -40000(1 - x/n) + 100T$, and $\theta_C = 640 - 45T$, also in units of deg cm^2 $dmol^{-1}$, where *T* is in °C, *x* is the number of residues in the chain, and *n* is constant used to correct for non-hydrogen-bonding carbonyls that do not contribute to θ_H (*14*).

Enzyme Kinetics. The ability of an elution fraction to confer activity against 2′3′CMP (*15*) upon S-protein was used to identify fractions containing Pep-1F and M13A-1F. The increase in absorbance at from 290 to 305 nm was followed for 60 s after adding 10−100 μL of an unknown fraction to a 1 mL solution containing 2.5 μM S-protein, 440 μM 2′3′CMP, and 100 mM acetic acid buffer, pH 4. The assays were done at ambient temperatures from 22 to 26 °C, and the baselines in the absence of added fraction were subtracted. Pep-1 was used as a positive control. The enzymatic activities with Pep-1F and M13A-1F are qualitatively similar to that with Pep-1. Reaction rates could also be measured in 10 mM MOPS, pH 6.7, 10 °C, by a stopped-flow assay in an Applied Photophysics SX-17 MV. Data taken in the first second were free from product inhibition. A fast increasing phase observed in the first 0.1 s may correspond to formation of an intermediate on the enzymatic reaction pathway.

Spectrophotometers. Absorbance measurements were made on a Hewlett-Packard 8452A diode array spectrophotometer, or a thermally regulated Kontron Uvikon UV/Vis spectrophotometer, and fluorescence measurements were made on Perkin-Elmer Lambda 5 or SLM-Aminco AB2 luminescence spectrometers. Both fluorometers were thermally regulated and stirred the samples. House air was passed over Drierite (Hammond) and through the sample

compartments to prevent condensation on cuvettes for experiments conducted at ≤10 °C. Fast reactions were measured by fluorescence or absorbance using a thermally regulated Applied Photophysics SX-17 MV stopped-flow spectrophotometer. The dead time of the instrument was found to be 2 ms with the reaction introduced by Tonomura et al. (*16*).

pH Titrations. The pK_a values of protons affecting the absorbance and fluorescence emission of fluorescein, Pep-1F, M13A-1F, and the S-peptide analogues bound to S-protein were determined by following the absorbance change at 496 nm, or the emission change, using an excitation wavelength of 496 nm (slit width 2 nm) and an emission wavelength of 520 nm (slit width 4−10 nm), as the pH was varied from 10 to 4. Three milliliter samples were initially buffered in 5 mM CAPS, 20 mM NH_4Ac, pH 10, and contained from 0.1 to 5 μM of the chromophore. Aliquots of a 0.5 M acetic acid solution were added to the sample solutions; the chromophore concentrations in the acetic acid and sample solutions were matched. Sample path lengths were 2 or 10 mm and photomultiplier voltages were typically 600 V.

Binding Titrations. The extent of reaction of Pep-1F and S-protein was monitored by the decrease in fluorescence emission at 520 nm after excitation at 496 nm. The fluorometer settings are as described above for the pK_a measurements. Stirred 3 mL samples containing 0.1−1 μM Pep-1F were titrated by addition of aliquots of a 10 μM S-protein stock solution; the chromophore concentrations in the S-protein and sample solutions were matched.

Measurement of the Association Reaction. The fluorescence emission time-courses for the association of Pep-1F or M13A-1F and S-protein were measured on the stopped-flow device described above. S-peptide analogue solutions (0.2−0.8 μM) were mixed with an equal volume of a 0.1−100 μM S-protein solution in the same buffer. Samples were illuminated at 496 nm with the monochromator slits set at 2 mm and the path length 2 mm. Light exiting the flow cell at 90° was monitored at all wavelengths. The photomultiplier voltage was set at 600 V for most experiments, and the voltage offset was typically 3 V, such that voltages of about 0 were obtained at the end of kinetic time courses.

Measurement of the Dissociation Reaction. RNaseS* solutions were incubated under the final experimental conditions for at least 1 h. S-peptide analogue concentrations were from 0.2 to 2 μM during the incubation period, and S-protein concentrations were 2-fold greater than those of the S-peptide analogues at all times. The dissociation of Pep-1F or M13A-1F from S-protein was detected by adding a large excess of unlabeled Pep-1 to the samples, and monitoring the increase in fluorescence emission with excitation at 496 nm. The labeled complex and Pep-1 solutions were in the same buffer. The amplitude and rate constant of the equilibration process were found to be independent of the Pep-1 concentration for excesses ≥500-fold for displacement of Pep-1F and ≥50-fold for displacement of M13A-1F. Kinetics were measured using the SLM-Aminco AB2 fluorometer, set as described above for the measurement of the extent of the complex formation, for dissociation rate constants <0.01 s^{-1}. Each time course was initiated by addition of about 100 μL of a concentrated Pep-1 stock to a continuously mixed 3 mL solution of labeled complex in a covered cuvette and compared to a simultaneously measured trace without Pep-1. The Applied Photophysics stopped-flow device, set as described above for the measurement of the association reaction, was used to measure dissociation rate constants ≥0.01 s^{-1}. Time courses were initiated by mixing the labeled complex with an equal volume of a Pep-1 solution and compared to sequentially measured traces without Pep-1.

Table 1: Spectrophotometric pK_a Values of Fluorescein, Fluorescein-Labeled S-peptide Analogues, and the Pep-1F/S-Protein Complex[a]

sample	pK_a values	
	water	10% TFE
fluorescein	6.49 ± 0.1	6.60 ± 0.01
Pep−1F	6.40 ± 0.02	
Pep-1F/S-protein complex	6.74 ± 0.03	
M13A-1F	6.40 ± 0.01	6.46 ± 0.02
fluorescein[b]	6.32 ± 0.01	

[a] From the change in emission of 1 μM chromophore at 520 nm with excitation at 496 nm at 10 °C unless otherwise noted. pK_a values are from fits of the Henderson−Hasselbach equation. [b] From the change in absorbance at 496 nm of 10 μM fluorescein at 25 °C.

Interrupted Refolding. The interrupted refolding assay was performed similarly to the assay for the dissociation rate constant, except that the M13A-1F/S-protein complex was allowed to associate for only a brief and precisely measured period of time before the addition of Pep-1. The Applied Photophysics stopped-flow device was used to mix sequentially and incubate M13A-1F and S-protein, mix the partially or fully folded complex with Pep-1, and follow the dissociation of M13A-1F by the increase in fluorescence emission. The stopped-flow device was set as described above for the measurement of the association reaction. The stopping syringe volume was set to 400 μL with the first and second push volumes being 220 and 180 μL, respectively. Mixing ratios 1:1 were used throughout. The concentrations in the flow cell were 0.2 μM M13A-1F, 1 μM S-protein, and 50 μM Pep-1, buffered in 10 mM MOPS, pH 6.7, at 10 °C.

RESULTS

Helicity of Pep-1F. The far-UV CD spectrum of Pep-1F is typical of a partially α-helical peptide in equilibrium with coil (*14*). The fraction helix was calculated (see Methods) using $n = 15$, $x = 2.5$, and a measured value of $\theta_{222} = -7.6 \times 10^3$ deg cm^2 dmol^{-1}. A portion of free Pep-1F is helical (21 (± 5)%) under strongly native conditions. The uncertainty results from the presence of aromatic groups in Pep-1F (*11*).

Spectral Changes Associated with Complex Formation. The difference spectrum for Pep-1F binding to S-protein is similar to that for FTC-labeled des-Lys-1 S-peptide binding to S-protein reported earlier (*13*). There is a 13% decrease in either the absorbance at 496 nM or the fluorescence emission at 520 nm after excitation at 496 nm. These changes are the result of an 0.34 ± 0.04 increase in the pK_a of the chromophoric proton of fluorescein (Table 1). The pK_a value of the M13A-1F variant is similar to that of Pep-1F. Trifluoroethanol promotes helix formation in soluble peptides (*17*). The effect of 10% TFE on the pK_a value of M13A-1F is similar to, or slightly smaller than, its effect on

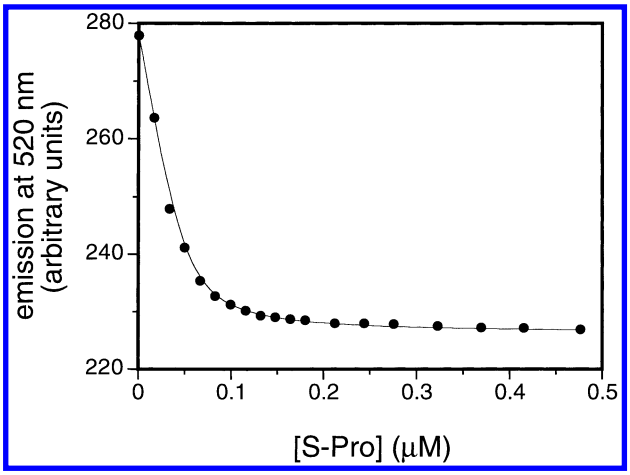

FIGURE 1: Equilibrium titration of 35 nM Pep-1F with S-protein at 31 °C and 100 mM ammonium acetate, pH 6.8. The sample was excited at 496 nm and emission was monitored at 520 nm in a fluorometer. The solid line is from fitting eq 3 with $K_d = 6 \pm 0.6$ nM.

free fluorescein, suggesting that the change in pK_a upon binding to S-protein is not caused by a change in helicity.

Binding of Pep-1F and S-protein at Equilibrium. The dissociation constant (K_d) of the Pep-1F/S-protein complex may be determined in conditions where binding is not too tight (see below) by titrating Pep-1F with S-protein and monitoring emission at 520 nm after excitation at 496 nm. A typical binding isotherm is shown in Figure 1, and K_d is determined from a fit of eq 3

$$F = \Delta F\{(K_d + p + N) - \mathrm{sqrt}[(K_d + p + N)^2 - 4pN]\}/2p \quad (3)$$

to the fluorescence intensity, F, where ΔF is the total change in fluorescence and p and N are the concentrations of Pep-1F and S-protein, respectively.

Kinetics of Association of the RNaseS Complex.* Under pseudo-first-order conditions ([S-protein] ≥ 5[Pep-1F]), a single exponential decrease in the emission of samples excited at 496 nM is observed in the stopped-flow spectrometer (Figure 2a). (A time course for dissociation under identical conditions is shown in Figure 2b; see below.) The pseudo-first-order rate constant for association (k_{obs}, s^{-1}) increases with the concentration of S-protein. For some Pep-1F stock solutions, a second, smaller, and more slowly decreasing phase is also observed (data not shown). It does not appear with the M13A-1F variant and we attribute it to the presence of peptide containing S^{δ} methionine sulfoxide, which is a frequently observed contaminant in S-peptide preparations. Reverse phase fast protein liquid chromatography (FPLC) chromatograms of the stock solutions display a minor peak (≤20%) eluting just before the main Pep-1F peak, consistent with presence of some oxidized peptide, when the second phase is seen.

k_{obs} is a linear function of the concentration of S-protein below 10 μM (Figure 3). The slope of such a plot is the bimolecular association rate constant, or k_{on}, where $k_{obs} = k_{on}$[S-protein] + k_{off}. The value of the slope under strongly native conditions and low ionic strength is $(1.82 \pm 0.08) \times 10^7$ M^{-1} s^{-1} and the intercept is -4 ± 10 s^{-1}, indicating $k_{off} < 6$ s^{-1}. Above 10 μM S-protein there is an apparent

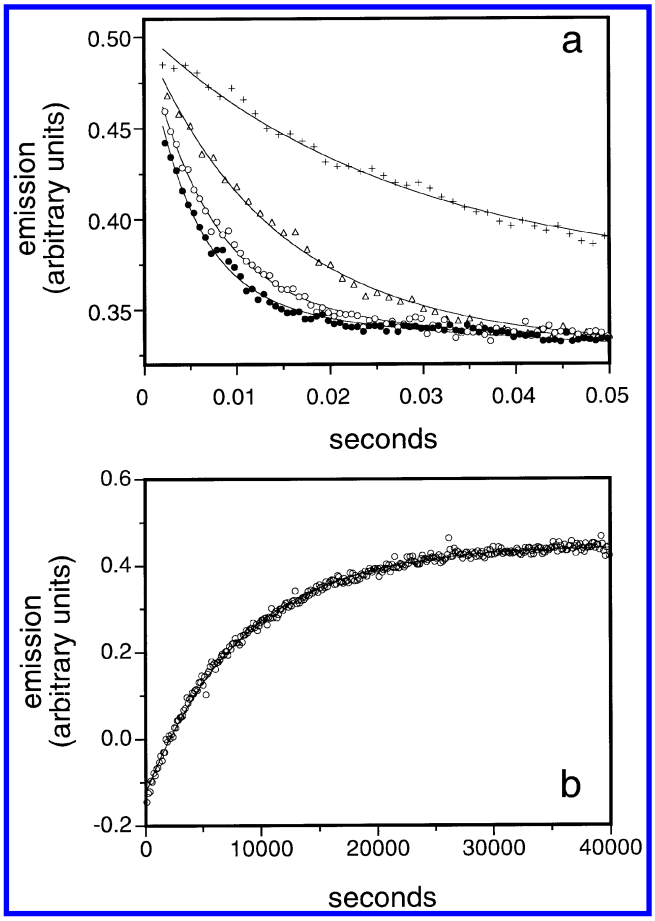

FIGURE 2: (a) Time course of emission after mixing of 0.4 μM Pep-1F and 2, +; 4, △; 8, ○; and 10, ● μM S-protein at 10 °C in 10 mM MOPS, pH 6.7, in a stopped-flow device. The sample was excited at 496 nm, and emission at all wavelengths was monitored at 90°. The data are fitted by single-exponential curves (solid lines). The pseudo-first-order rate constants from the fits are defined as k_{obs} with units of s^{-1}. (b) Time course of emission after mixing 0.2 μM of the complex between Pep-1F and S-protein with 200 μM unlabeled Pep-1. The other conditions are identical to (a). The sample is excited at 496 nm, and emission at 520 nm is monitored. The time course is fitted by a single-exponential curve (solid line). The observed first-order rate constant of $(1.19 \pm 0.08) \times 10^{-4}$ s^{-1} is k_{off}, the dissociation rate constant for the complex.

leveling-off of k_{obs}. This leveling-off may be a consequence of saturation of a rapidly formed intermediate on the folding/association pathway. In this case it is appropriate to model the data with the mechanism

$$p + N \underset{k_{21}}{\overset{k_{12}\,[\text{S-pro}]}{\rightleftharpoons}} I_r \xrightarrow{k_{23}} pN \quad (4)$$

and the Michaelis−Menten approximation, that is, $k_{obs} = k_{23}/(1 + K_M/[\text{S-pro}])$, where $K_M = (k_{21} + k_{23})/k_{12}$. p, N, and pN are defined in eq 1, and I_r is an intermediate. The parameters obtained from fitting the entire range of data in Figure 3 to this model are $K_M = 18 \pm 1$ μM and $k_{23} = 390 \pm 80$ s^{-1}. The value of k_{23} is within the range that may be reliably measured by stopped-flow spectrophotometry given the instrumental dead time of 2 ms. The bimolecular association rate constant for complex formation in this approximation (k_{23}/K_M) corresponds to k_{on} and has a value of $(2.1 \pm 0.5) \times 10^7$ M^{-1} s^{-1}, which is 18% greater than k_{on} from the linear model. The k_{on} values reported here are calculated by the linear model using data acquired at and

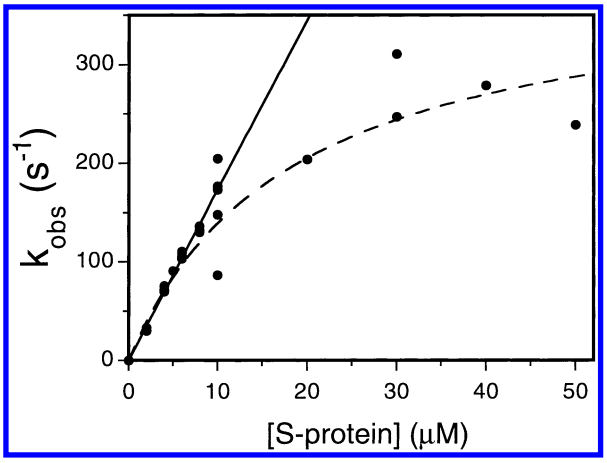

FIGURE 3: Dependence on S-protein concentration of the pseudo-first-order rate constants (k_{obs}). The conditions are as described in Figure 2a. The slope of the straight line through the points below 10 μM S-protein is equal to the bimolecular association rate constant for the complex (k_{on}). Here $k_{on} = (1.82 \pm 0.08) \times 10^7$ M^{-1} s^{-1}. The curved line is a fit of the Michaelis−Menten model to the data and the fitted parameter values are in given the text.

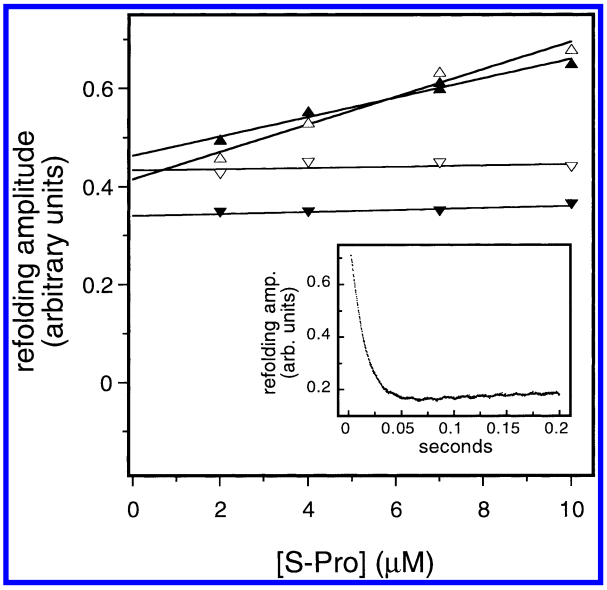

FIGURE 4: Amplitudes for the association reactions of M13A-1F and S-protein as a function of the concentration of S-protein at (△) 1.7 °C; (▲), 9.7 °C, (▼) 19.3 °C, and (▽) 29.0 °C. The conditions are as described in Figure 2a except for the variation in temperature. Inset: refolding time course for M13A-1F and 10 μM S-protein at 1.7 °C showing the second, slower increasing phase.

below 10 μM S-protein. Importantly, the effects of varying the reaction conditions upon k_{on} calculated by either model are expected to be very similar.

Temperature Dependence of Apparent Complexity in the Association Reaction. At and above 10 °C there is a single decreasing phase after mixing S-peptide analogue and S-protein in the stopped-flow spectrophotometer (Figure 2a), except in the presence of contaminating oxidized S-peptide as described above. Below 10 °C a small (≤20%) increasing phase is observed at and above 7 μM S-protein (Figure 4, inset). The time constant for this minor phase, which is observed for both Pep-1F and M13A-1F, is 23 ± 10 s^{-1}. The amplitude of the major decreasing phase observed after mixing M13A-1F with S-protein increases as the concentration of S-protein is increased at 1.7 and 9.7 °C, 10 mM MOPS, pH 6.7 (Figure 4). At 19.3 and 29 °C this increase

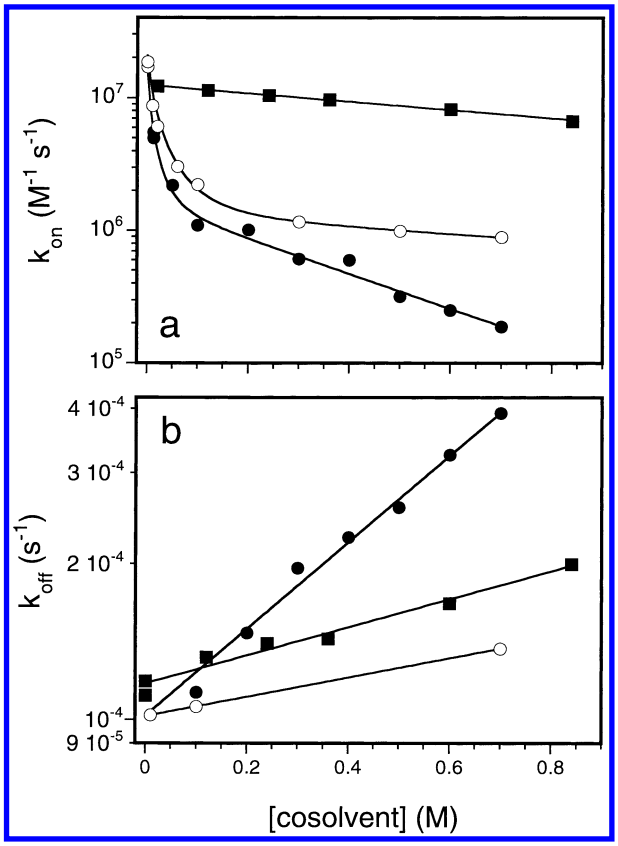

FIGURE 5: Effects of (●) GdmCl, (■) urea, and (○) NaCl on (a) k_{on} and (b) k_{off}. The conditions are as described in Figure 2a (a) and Figure 2b (b) except for the presence of cosolvent. The curved lines through the GdmCl and NaCl data in (a) are from fits of eq 5. The straight lines through the other data are from fits of a single-exponential model (*i.e.*, eq 5, with n set to 0). The fitted parameters are in Table 2.

is absent (Figure 4), as it is at 10 °C above 0.3 M NaCl or GdmCl (data not shown). Similar behavior is observed for the reaction of Pep-1F and S-protein.

The Dissociation Reaction. The dissociation rate constant (k_{off}) is determined directly in a competition experiment. A quantity of the labeled RNaseS* complex (0.1−1 μM) is mixed with a vast excess of unlabeled Pep-1, and the emission time course is monitored (Figure 2b). A sufficient excess of unlabeled peptide ensures that the concentration of free S-protein, and therefore the rate of reassociation of Pep-1F and S-protein, is small. k_{obs} is independent of the concentration of unlabeled peptide for concentration excess >500-fold. Therefore, k_{obs} from fitting a single exponential to the data in Figure 2b is very similar to k_{off}.

Dependence of Kinetic Parameters on Denaturant and Salt Concentration. The effects of urea and NaCl concentration on the rate constants for association and dissociation of the complex were measured over a range of concentrations well below the unfolding transition of S-protein (*18*). The effects of GdmCl were measured at concentrations below the midpoint of the unfolding transition for S-protein according to unpublished data (F. X. Schmid & R. L. Baldwin, taken in similar conditions, pH 6, 10 °C). k_{on} is plotted against the concentration of cosolvent for GdmCl, urea, and NaCl in Figure 5a, and k_{off} for the same series and concentration range is plotted in Figure 5b. There is a strong decrease of k_{on} with increasing concentration of GdmCl and NaCl from 0 to 300 mM, which is probably caused by ionic screening

Table 2: Kinetic and Equilibrium Parameters for the Effects of GdmCl, Urea, and NaCl on the Reaction of Pep-1F and S-Protein[a]

	GdmCl	urea	NaCl
k_{on}^0 (M^{-1} s^{-1})	$(1.7 \pm 0.3) \times 10^{6}$ [b]	$(1.2 \pm 0.1) \times 10^{7}$ [c]	$(1.4 \pm 0.4) \times 10^{6}$ [c]
m_{on} (kcal mol^{-1} M^{-1})	-1.6 ± 0.2[b]	-0.41 ± 0.02[c]	-0.4 ± 0.3[c]
n[b]	28 ± 4		23 ± 7
C[b]	-20 ± 2		-12 ± 1
k_{off}^0 (s^{-1})[c]	$(1.01 \pm 0.04) \times 10^{-4}$	$(1.20 \pm 0.03) \times 10^{-4}$	$(1.01 \pm 0.04) \times 10^{-4}$
m_{off} (kcal mol^{-1} M^{-1})[c]	1.09 ± 0.05	0.34 ± 0.03	0.24 ± 0.03
m_{eq} (kcal mol^{-1} M^{-1})[d]	2.8 ± 0.3	0.75 ± 0.04	0.64 ± 0.3

[a] The conditions are 10 mM MOPS, pH = 6.7 ± 0.15, $T = 10 \pm 0.2$ °C except for the presence of the cosolvent. [b] From the fit of eq 5 to k_{on} in the presence of GdmCl and NaCl (Figure 5a). [c] From a fit of eq 5 (with n set to 0) to k_{on} for NaCl (>0.3 M) and urea (>0 M) (Figure 5a) and k_{off} for urea (entire range) or GdmCl and NaCl (>0 M) (Figure 5b). [d] The equilibrium m-value, $m_{eq} = m_{on} - m_{off}$.

of the electrostatic attraction between the S-peptide analogue (charge ≈ −2.5) and S-protein (charge ≈ +4.5) at neutral pH. After saturation of this effect, there is a linear decrease in the logarithm of k_{on} with [cosolvent] (Figure 5a), as is observed also for urea. Similarly, there is a linear increase in the logarithm of k_{off} with increasing concentration of each of the three cosolvent species, but for k_{off} there is no screening effect at low ionic strength (Figure 5b).

The solid lines in Figure 5 are obtained by fitting eq 5 to the data,

$$k = k^0 \exp(m^{\ddagger}/RT[\text{cosolvent}]) + nk^0 \exp(CI^{0.5}) \quad (5)$$

where k is either an association or dissociation rate constant, and k^0 and $m^{\ddagger}$ (m_{on} or m_{off}) are the intercept and slope terms, respectively, of the linear portions of the logarithm k vs [cosolvent] plots. The form of the second term on the right is based on the Debye−Hückel theory for simple systems, where n is the factor by which the charge of the reactants changes the rate constant, C is a constant, and I = ionic strength.[2] k_{on}^0 for GdmCl and NaCl provides an estimate of the rate constant at zero denaturant concentration for the hypothetical neutral reactants, since the charges are nearly fully screened at $I \geq 0.1$. k_{on}^0 for urea and k_{off}^0 for all three cosolvents species were determined with n set to 0, since there is no effect of ionic strength on k_{on} with urea or with any cosolvent on k_{off}. The data points at 0 M cosolvent for k_{on} with urea and for k_{off} with GdmCl and NaCl were not included in the analysis. The small $m^{\ddagger}$ value for k_{on} in the presence of NaCl is swamped by the large ionic strength effect. Therefore, k_{on}^0 and $m^{\ddagger}$ are determined from fitting eq 5 with $n = 0$ to the linear portion of the data set ([NaCl] ≥ 0.3 M). The fitted values of k^0 $m^{\ddagger}$, n, and C are given in Table 2.

The weighted averages of n, k^0, and C for GdmCl and NaCl are 26 ± 5, $(1.6 \pm 0.3) \times 10^6$ M^{-1} s^{-1}, and −16 ± 4, respectively. The hypothetical rate constant at zero ionic strength is $(4.2 \pm 1) \times 10^7$ M^{-1} s^{-1}, and the ionic strength effect on k_{on} (expressed as $-RT \ln n$), is 1.8 ± 0.3 kcal mol^{-1}.

Cosolvent Effects on the Dissociation Constant. For two-state complex formation the equilibrium dissociation constant, $K_d = k_{off}/k_{on}$. Values of K_d for which k_{off} and k_{on} were measured under identical conditions are plotted against [cosolvent] in Figure 6a. Parameters obtained from fitting eq 5 to the kinetic data were used to calculate k_{on} and k_{off} as functions of [cosolvent], and the solid lines in Figure 6a are the ratios of these calculated values. The value of K_d extrapolated to zero ionic strength is 3 ± 0.8 nM (−15 ± 0.2 kcal mol^{-1}). The difference between the kinetic m-values ($m_{on} - m_{off}$), is the equilibrium m-value (Table 2).

[2] I = [cosolvent] + 0.0029 for the cosolvents GdmCl and NaCl, where the ionic strength contributed by 10 mM MOPS at pH 6.7 = 0.0029.

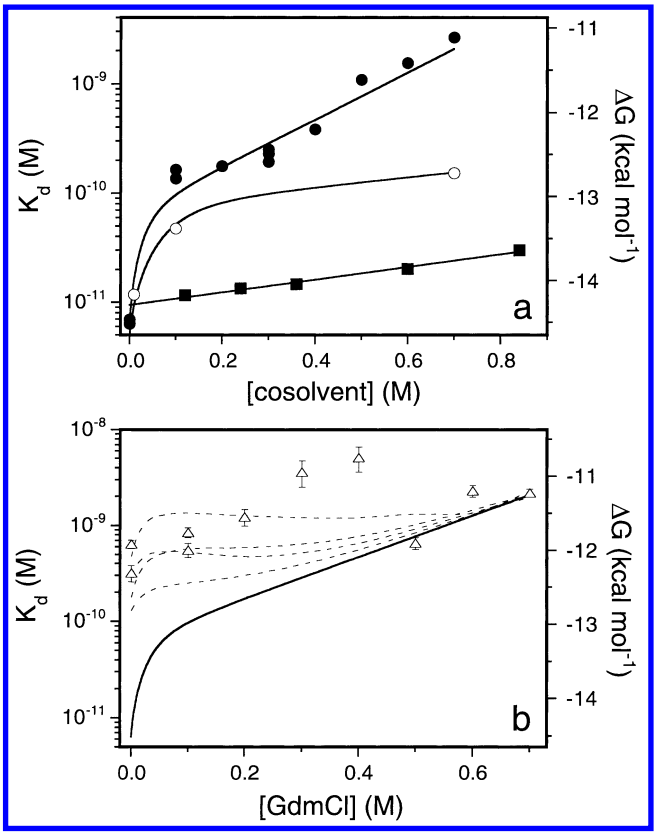

FIGURE 6: Apparent dissociation constant (K_d, left axis, $\Delta G = -RT \ln K_d$, right axis, T = 283 K) for the RNaseS* complex (Pep-1F) as a function of cosolvent concentration. The conditions are as described in Figure 2 except for the presence of cosolvent. (a) The kinetically determined values of K_d ($=k_{off}/k_{on}$) are shown in the presence of (●) GdmCl, (■) urea, and (○) NaCl. The standard errors are approximately the size of the data points. The solid lines through the data are calculated from eq 5 using the parameters in Table 2 as described in the text. (b) The apparent value of K_d measured by the equilibrium titration method, △, as a function of the GdmCl concentration. The solid line is the dissociation constant calculated from kinetic data, as described in (a), and is shown for comparison. The dashed lines are drawn through K_d values from simulated equilibrium titrations in which Pep-1F is supposed to contain 5% or 10% of a weakly binding contaminant, as described in the text.

K_d values measured by the equilibrium titration method at 10 °C, 10 mM MOPS, pH 6.7, as a function of [GdmCl], are plotted in Figure 6b. The values calculated from the kinetic data in GdmCl are shown for comparison (solid line).

The kinetic and equilibrium values of K_d are very similar at GdmCl concentrations at or above 0.5 M, indicating that the reaction behaves as a clear-cut two-state reaction under slightly destabilizing conditions. A similar result is obtained when RNaseS* is slightly destabilized by temperature. The value of K_d determined kinetically at 31 °C in 0.1 M NH_4-Ac, pH 6.8, is 4.2 ± 0.5 nM, similar to the value of 6 ± 0.6 nM measured by titration under identical conditions (Figure 1). Below 0.5 M GdmCl at 10 °C, the kinetic K_d values are significantly smaller than the equilibrium values.

Simulated Dissociation Constants. We simulated titration curves in the presence of hypothetical damaged peptide in order to determine whether this effect can explain the difference between the kinetic and equilibrium K_d values in Figure 6b. Binding isotherms were simulated using eq 3 to calculate the extent of reaction of a mixture containing 95 or 90% of a strongly binding peptide (K_d = 6 pM) and 5 or 10% of a species with K_d increased (binding is weakened) by 6000-fold.[3] Equation 3 was then fitted to the simulated data using a range of S-protein concentrations up to 0.5 or 2 μM. The effect of GdmCl on the simulated isotherms was introduced by applying the *m*-values from the kinetically determined K_d values (Table 2), and the same *m*-value was applied to both the strongly and weakly binding populations. The simulated K_d values (Figure 6b, dashed lines) are overestimated under strongly stabilizing conditions but are accurate under slightly destabilizing conditions. The simulated titrations thus bear the same relationship to the kinetic data as do the equilibrium data.

Pep-1F Binds to S-protein with Remarkably High Affinity. The dissociation constant for Pep-1F and S-protein measured kinetically is 6 pM at 10 °C in 10 mM MOPS, pH 6.7. For S-peptide at 0 °C in 0.12 M sodium cacodylate, pH 6.4, K_d measured by hydrogen exchange is 220 pM (*19*). The greater stability of RNaseS* with Pep-1F ($\Delta\Delta G = -2.4$ kcal mol^{-1}) may be rationalized as follows. (a) The complex becomes more stable at higher pH (*19*). (b) The difference in net charge between Pep-1F and S-protein (about 7) stabilizes the complex by about 1.4 kcal mol^{-1}. There is little difference in net charge between wild-type S-peptide and S-protein at neutral pH. (c) The substitution of acetyl-Tyr for Lys-1 reduces the positive charge near the N-terminus of the S-peptide, and the change is expected to help stabilize the complex by about 0.16 kcal mol^{-1} (*20*). (d) Fluorescein on Lys-7 of des-1 S-peptide stabilizes RNaseS by 1.2 kcal mol^{-1} (*13*). The combined differences between Pep-1F and S-peptide are sufficient to explain the difference in their K_d values.

Evidence for Two Intermediates on the Folding Pathway of RNaseS. The First Intermediate.* The leveling off of k_{obs} at high concentrations of S-protein (Figure 3) might be ascribed to saturation of a reaction intermediate or, instead, to aggregation of S-protein, since 170 μM S-protein exists as hexamers in 5 mM Tris, pH 8.0, 100 mM NaCl (*21*). Sedimentation equilibrium data for S-protein in 10 mM MOPS, pH 6.8, 10 °C, indicate that S-protein is a monomer at all concentrations used in our kinetics assays (J.M.G. and R.L.B., unpublished data). Therefore, the most likely explanation for the saturation of k_{obs} at high concentrations of S-protein is the existence of a rapidly formed intermediate on the refolding pathway of RNaseS* (I_r in eqs 4 and 6, and Figure 7). Our study was made at a lower ionic strength, and also at a pH value farther from the isoelectric point of S-protein, than was that of Allende and Richards (*21*). Both of these differences are expected to reduce the tendency of S-protein to aggregate.

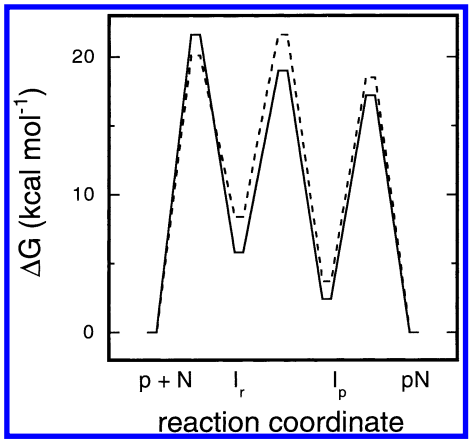

FIGURE 7: Free energy profiles for the formation and dissociation of RNaseS* at 10 °C, 10 mM MOPS, pH 6.7 (eq 6). The solid and dashed lines depict the limiting cases in which reaction is respectively encounter-limited or folding-limited. The choice of mechanism, and calculation of the barrier heights are described in the text. The relative position of p + N and the first barrier depend on the concentration of N; 6 pM, the K_d value for complex formation, was our arbitrary choice.

The small linear increase in the main refolding amplitude with increasing S-protein at and below 10 °C (Figure 4) is also consistent with the presence of a transient intermediate on the refolding pathway (I_r in eqs 4 and 6, and Figure 7). This intermediate must have greater fluorescence emission than the free S-peptide analogue and reach dynamic equilibrium in the dead time of a stopped-flow experiment. The amplitude anomaly cannot be explained by changes in the extent of reaction of S-peptide analogues and S-peptide at equilibrium, since >0.99 of the S-peptide analogue would form complex at the lowest S-protein concentration even if K_d were as high as 1 nM. Furthermore, the increase in amplitude is not caused by an additional reaction with the M13-sulfoxide S-peptide analogue, since the increase is also observed with M13A-1F, which lacks methionine.

The Second Intermediate. The small increasing phase which occurs in the refolding reaction of Pep-1F and M13A-1F below 10 °C and above 7 μM S-protein (Figure 4, inset) suggests the presence of an intermediate which occurs late on the refolding pathway (I_p in eq 6 and Figure 7). This intermediate must occur after the committed step in refolding since the rate constant for the second phase is 23 s^{-1}, while the dissociation rate constant for this species returning to free S-peptide analogue and S-protein can be no higher than 6 s^{-1}, as estimated from the intercept of Figure 3. This intermediate breaks down more slowly than the first intermediate described above, and therefore must come later in refolding. It is possibly a nativelike isomer of RNaseS*. Proline isomerization is not a likely explanation for this phase since S-protein is folded before mixing with S-peptide.

Free Energy Profile of the Reaction. Free energy profiles for the formation and dissociation of RNaseS* at 10 °C, 10

[3] The effect on K_d of Met-13 oxidation is estimated to be 6000-fold (see Figure 1 in the following article, compare K_d for H12A-1F and H12A/M13 sulfoxide-1F).

mM MOPS, pH 6.7 are shown in Figure 7. The barrier heights are calculated from $\Delta G^{\ddagger} = -RT \ln[k/(k^{\ddagger})]$, where $k^{\ddagger}$ is a prefactor and k is the observed rate constant. The value of the prefactor for protein folding reactions is unknown, and we use the standard Eyring prefactor (k_BT/h), where h is Planck's constant and k_B is the Boltzmann constant, without implying that it is the correct prefactor in protein folding reactions. The relative position of p + N and the transition state for formation of I_r depends on concentration of N. Our arbitrary choice was 6 pM, the K_d value for RNaseS* formation.

The microscopic rate constants are defined in eq 6

$$p + N \underset{k_{21}}{\overset{k_{12}[N]}{\rightleftharpoons}} I_r \underset{k_{32}}{\overset{k_{23}}{\rightleftharpoons}} I_p \underset{k_{43}}{\overset{k_{34}}{\rightleftharpoons}} pN \qquad (6)$$

where p, N, and pN are introduced in eq 1. I_r is an intermediate which forms in the dead time of a stopped-flow experiment and has greater fluorescence emission than p. I_r is less than 25% populated below 10 μM S-protein. I_p is an intermediate in rapid equilibrium with product and has a lower fluorescence emission than pN.

The reaction may be encounter-limited (Figure 7, solid line) or folding-limited (Figure 7, dashed line). In the former case k_{12} is the measured value of k_{on} (1.8×10^7 M^{-1} s^{-1}; Figure 3) and k_{21} is arbitrarily set to 3.9 s^{-1}. In the latter case k_{12} is taken as 3×10^8 M^{-1} s^{-1}, the largest rate constant measured for a bimolecular protein folding reaction (*7*), and the estimated value of k_{21} is K_M k_{12} = 5400 s^{-1} (see eq 4). In either case k_{23} = 390 s^{-1}, the saturating value of k_{obs} (Figure 3), and k_{34} = 23 s^{-1}, from the small increasing phase (Figure 4, inset). k_{32} and k_{43} are set to 1 s^{-1} and 0.23 s^{-1}, respectively, for the encounter-limited model, or to 0.1 s^{-1} and 0.023 s^{-1}, respectively, for the folding-limited model, so that k_{off} is 0.0001 s^{-1} (Figure 2b).

Interrupted Refolding of the M13A-1F/S-protein Complex. We measured the rate of formation of native M13A-1F/S-protein complex by an unfolding kinetics assay in an interrupted refolding experiment (*22*). The aim is to determine whether the reaction monitored by the major fluorescence emission phase (Figure 8, left axis) is formation of the native protein or a less stable intermediate. We chose the mutant RNaseS* containing M13A-1F rather than Pep-1F because the unfolding of the former complex may be measured more conveniently. The complex dissociates in a single kinetic phase at all refolding times, and the rate is similar to that observed when the complex has been refolded for several hours. Thus, the amplitude of the unfolding reaction (Figure 8, right axis) is directly proportional to the extent of complex formation at each time in refolding. The amplitude of the unfolding reaction is equal in magnitude and opposite in sign to the amplitude measured in refolding at each time; therefore, the major fluorescence emission phase observed for refolding corresponds to formation of the native complex.

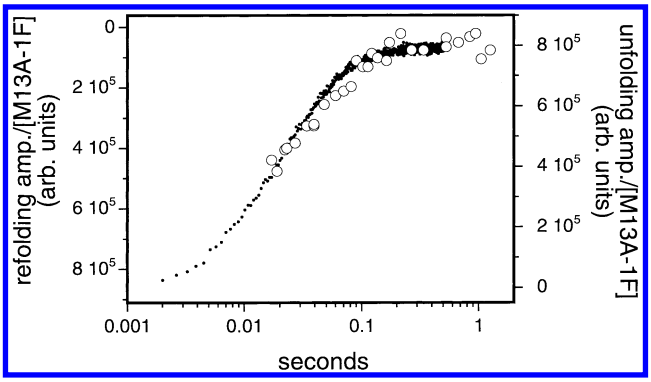

FIGURE 8: Right axis (○): the amplitude/[M13A-1F] of the unfolding reaction of the M13A-1F/S-protein complex after refolding for the indicated time at 10 °C, 10 mM MOPS, pH 6.7. Refolding takes place in the presence of 0.4 μM M13A-1F and 2 μM S-protein, and the concentrations during unfolding are 0.2 M M13A-1F, 1 μM S-protein, and 50 μM Pep-1. The amplitude of the unfolding reaction is directly proportional to the extent of native complex formation. The rate constant and normalized amplitude for native complex formation are 33 ± 1.7 s^{-1} and 79 000 ± 10 000 M^{-1}, respectively. Left axis (●): the amplitude/[M13A-1F] of a simple refolding experiment under identical conditions. The concentrations of M13A-1F and S-protein are 0.4 and 2 μM S-protein, respectively. The observed rate constant and normalized amplitude are 35.6 ± 0.3 s^{-1} and −77 000 ± 4000 M^{-1}, respectively.

DISCUSSION

Formation of RNaseS is Described by the Two-State Approximation.* An important advantage of the RNaseS* system is that formation and dissociation of the complex are monitored under identical strongly native conditions. The appearance of pN measured in an interrupted refolding experiment mirrors the disappearance of p (p = M13A-1F) (Figure 8), indicating that the reaction may be described by the two-state approximation at low concentrations of S-protein. This means that the stability of the complex may be calculated directly from the two rate constants. The two-state behavior of the system was also confirmed by comparing the K_d value for Pep-1F calculated from the rate constants to that measured by an equilibrium technique (Figure 6b). The kinetic and equilibrium K_d values are identical under slightly destabilizing conditions, and the disagreement between the kinetically and directly measured values of K_d below 0.5 M GdmCl is readily explained by the limitations of the equilibrium assay and the presence of a small fraction of oxidized S-peptide (*19*). The reliable measurement of K_d allows us to use transition state theory to describe quantitatively the docking and refolding of S-peptide with folded S-protein in terms of the extent of formation of nativelike interactions in the activated complex.

Association and Folding of RNaseS Has a Large Free-Energy Barrier.* The packing of a single helix in the context of an otherwise folded protein might be expected to be a very fast reaction, perhaps even lacking a free energy barrier sufficient for the application of transition state theory (*3*). The bimolecular nature of the RNaseS* reaction inserts a translational entropy barrier into the process, which will lead to two-state kinetics even if other barriers are low. This barrier corresponds to the p + N to I_r step in Figure 7. The leveling off of k_{obs} beginning at about 10 μM S-protein (Figure 3) indicates that the encounter of S-peptide and S-protein is followed by another significant free energy barrier, described by a first-order rate constant of 390 ± 80 s^{-1}, corresponding to the I_r to I_p step in Figure 7, and with $\Delta G^{\ddagger}$ = 13.2 kcal mol^{-1}. The properties of this unexpected free energy barrier, and of the intermediate which accumulates at high concentrations of S-protein, must be characterized in future studies.

Ionic Strength Effects. Screening the charges on Pep-1F and S-protein reduces k_{on} by a factor of 26 ± 4 but has little effect on k_{off} (Figure 5, Table 2), indicating that the separation of charges at the transition barrier is nativelike. A similar behavior has been observed for the folding of a leucine zipper (*23*) and for the binding of barstar to barnase (*24*). The formation of RNaseS* may be either encounter-limited or folding-limited (Figure 7). Unfortunately, the ionic strength data do not distinguish between these models. The Smoluchowski equation for an encounter-limited reaction, modified to account for ionic strength effects on the kinetics of association (*25*) and dissociation (*26*) of charged reactants, predicts that k_{on} but not k_{off} will change as a function of the square root of the ionic strength, and this is what we observe. The reduction in k_{on} could also be caused, however, by reduction of the concentration of a charge-stabilized intermediate (I_r in Figure 7 and eqs 4 and 6) which depends on ionic strength; note that for the folding-limited case in Figure 7 I_r occurs before the rate-determining step. Ionic strength would not affect k_{off} in this case, since the hypothetical intermediate occurs after the rate-determining step for dissociation.

k_{on}^0, the extrapolated value of the bimolecular association rate constant in the absence of charge effects, is 1.6×10^6 M^{-1} s^{-1} (eq 5, Table 2). This is about an order of magnitude larger than the value for reaction between neutral barstar and barnase (*24*, *27*, *28*), but it is 2 orders of magnitude smaller than the second-order rate constant for refolding of the neutral MYL mutant of Arc-repressor dimer (*7*). This set of results indicates, surprisingly, that unfolded and partially unfolded proteins may combine more rapidly than folded proteins in the absence of ionic steering effects. A possible explanation is that geometric restrictions on the reaction (*29*, *28*) are relaxed for unfolded proteins and that folding may be faster than the reorientation of rigid macromolecules. The charge effect on the association rate constant of S-peptide analogues and S-protein is smaller than that for barnase and barstar (*24*). The largely disordered S-peptide analogue has little permanent dipole moment; therefore, rotational ionic steering effects (*28*) cannot guide this reaction.

There is a small but significant decrease in the value of k_{off} as the chloride concentration is increased from 0 to 0.1 mM with either GdmCl or NaCl (Figure 5b). This is consistent with stabilization of RNaseS by anion binding (*30*).

Denaturant Dependence of the Association and Dissociation Rates. The slope, or *m*-value, of a plot of ln *K* vs [cosolvent] is considered to be proportional to the extent of protein surface area buried in a folding transition (*31*), where the sites for interaction with denaturant are likely to be predominantly peptide CO and NH groups, at least in the case of urea (*32*). Our kinetic assay detects the relative change in the number of these sites as p and N (refolding) and pN (unfolding) form the activated complex. Refolding and unfolding for a bimolecular system may be measured at very low denaturant concentrations, since jumps in the concentration of denaturant are not required to initiate the reactions; moreover, the *m*-values for k_{on} and k_{off} may be measured under identical conditions. Therefore, little extrapolation is required to infer the properties of the transition barrier species in the absence of denaturant and, importantly, the identical transition state are probed from both sides.

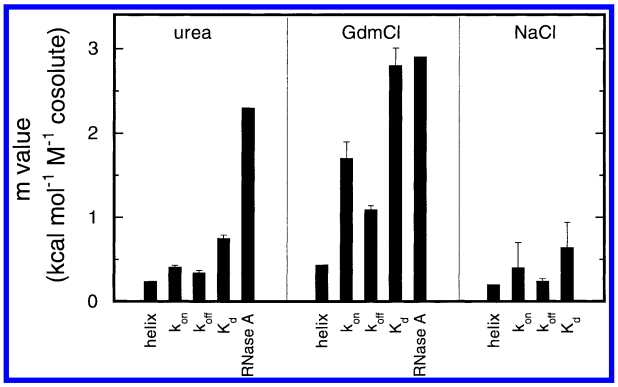

FIGURE 9: Effects (*m*-values) of urea, GdmCl, and NaCl on k_{on}, k_{off}, and K_d (k_{off}/k_{on}) for the Pep-1F/S-protein complex (Table 2). The data are compared to the *m*-value for the unfolding of RNase A from Pace and co-workers (*34*), and the m-value for unfolding a 10 residue alanine-based helix calculated from the parameters of Smith and Scholtz (*37*).

The ratio $m_{on}/m_{eq} = 0.57 \pm 0.1$ and 0.54 ± 0.04 for GdmCl and urea, respectively, which indicates that 55% of the sites interacting with denaturant that are buried in refolding are also buried in the transition state. The agreement between the ratios measured in GdmCl and urea is encouraging. The value of m_{on}/m_{eq} for S-peptide/S-protein recombination is close to the average value of 0.59 for the refolding of small monomolecular and bimolecular systems (*2*). The GCN4-p1 coiled-coil is the system most closely related to ours, being bimolecular and relatively small, and its value is also 0.55 (*33*).

The *m*-value for forming RNaseS* can be compared to that for RNase A refolding (*34*). The change in the accessible surface area associated with folding extended S-peptide to its native conformation and docking it to native S-protein is $^1/_3$ of that for refolding RNase A (*35*, *36*). If the *m*-value is proportional to the buried surface area, then the *m*-value for S-peptide/S-protein complex formation ought to be $^1/_3$ of that for refolding RNase A. This is precisely what we observe for urea, but the *m*-value derived from K_d in GdmCl is the same as that for unfolding RNase A (Figure 9). A plausible explanation is that S-protein begins to unfold at the low concentrations of GdmCl where our reaction is measured: the midpoint of the S-protein unfolding transition is 0.8 M GdmCl at pH 6.0, 10 °C (F. X. Schmid & R. L. Baldwin, unpublished).

The value of m_{on} for S-peptide binding to S-protein in urea exceeds that for formation of a 10-residue alanine-based helix (Figure 9; *37*, *32*). Therefore, helix formation by S-peptide cannot fully account for the value of m_{on}. The potential role of helix in stabilizing the activated complex is further discussed in the next article. We have no explanation for the significant drop in k_{on} between 0 and 0.02 M urea (Figure 5a).

ACKNOWLEDGMENT

We thank Dr. Douglas Laurents for valuable scientific discussions and Dr. David Baker for preprints of his manuscripts.

REFERENCES

1. Schindler, T., Herrier, M., Marahiel, M. A., and Schmid, F. X. (1995) *Nat. Struct. Biol. 2*, 663−673.

2. Scalley, M. L., Yi, Q., Gu, H., McCormick, A., Yates, J. R., and Baker, D. (1997) *Biochemistry 36*, 3373−3382.
3. Bryngelson, J. D., Onuchic, J. N., Socci, N. D., and Wolynes, P. G. (1995) *Proteins: Struct., Func., Gen. 21*, 167−195.
4. Zwanzig, R. (1995) *Proc. Natl. Acad. Sci. U.S.A. 92*, 9801−9804.
5. Scalley, M. L., and Baker, D. (1997) *Proc. Natl. Acad. Sci. U.S.A. 94*, 10636−10640.
6. Doyle, R., Simons, K., Qian, H., and Baker, D. (1997) *Proteins: Struct., Func., Gen. 29*, 282−291.
7. Jonsson, T., Waldburger, C. D., and Sauer, R. T. (1996) *Biochemistry 35*, 4795−4802.
8. Richards, F. M., and Vithayathil, P. J. (1959) *J. Biol. Chem. 234*, 1459−1465.
9. Hearn, R. P., Richards, F. M., Sturtevant, J. M., and Watt, G. D. (1971) *Biochemistry 10*, 806−817.
10. Wyckoff, H. W., Tsernoglou, D., Hanson, A. W., Knox, J. R., and Richards, F. W. (1970) *J. Biol. Chem. 245*, 305−328.
11. Chakrabartty, A., Kortemme, T., Padmanabhan, S., and Baldwin, R. L. (1993) *Biochemistry 32*, 5560−5565.
12. Cantor, C. R., and Schimmel, P. R. (1980) *Biophysical Chemistry II*, W. H Freeman, New York, p 377.
13. Labhardt, A. M., Ridge, J. A., Lindquist, R. N., and Baldwin, R. L. (1983) *Biochemistry 22*, 321−327.
14. Scholtz, J. M., Qian, H., York, E. J., Stewart, J. M., and Baldwin, R. L. (1991) *Biopolymers 31*, 1463−1470.
15. Crook, E. M., Mathias, A. P., and Rabin, B. R. (1960) *Biochem. J. 74*, 234−238.
16. Tonomura, B., Nakatani, H., Ohnishi, M., Yamaguchi-Ito, J., and Hiromi, K. (1978) *Anal. Biochem. 84*, 370−383.
17. Luo, P., and Baldwin, R. L. (1997) *Biochemistry 36*, 8413−8421.
18. Sherwood, L. M., and Potts, J. T., Jr. (1965) *J. Biol. Chem. 240*, 3799−3809.
19. Schreier, A. A., and Baldwin, R. L. (1977) *Biochemistry 16*, 4203−4209.
20. Mitchinson, C., and Baldwin, R. L. (1986) *Proteins: Struct., Func., Gen. 1*, 23−33.
21. Allende, J. E., and Richards, F. M. (1962) *Biochemistry 1*, 295−304.
22. Schmid, F. X. (1983) *Biochemistry 22*, 4690−4696.
23. Wendt, H., Leder, L., Härmä, H., Jelesarov, I., Baici, A., Bosshard, H. R. (1997) *Biochemistry 36*, 204−213.
24. Schreiber, G., and Fersht, A. R. (1996) *Nat. Struct. Biol. 3*, 427−431.
25. Debye, P. (1942) *Trans. Electrochem. Soc. 82*, 265−272.
26. Eigen, M., Kruse, W., Maass, G., and De Maeyer, L. (1964) *Progress in Reaction Kinetics* (Porter, G., Ed.) Vol. 2, pp 285−318, Macmillan, New York.
27. Gabdoulline, R. R., and Wade, R. C. (1997) *Biophys. J. 72*, 1917−1929.
28. Janin, J. (1997) *Proteins: Struct., Func., Gen. 28*, 153−161.
29. Hill, T. L. (1975) *Proc. Natl. Acad. Sci. U.S.A. 72*, 4918−4922.
30. Matthew, J. B., and Richards, F. M. (1982) *Biochemistry 21*, 4989−4999.
31. Schellman, J. A. (1978) *Biopolymers 17*, 1305−1322.
32. Scholtz, J. M., Barrick, D. B., York, E. J., Stewart, J. M., and Baldwin, R. L. (1995) *Proc. Natl. Acad. Sci. U.S.A. 92*, 185−189.
33. Sosnick, T. R., Jackson, S., Wilk, R. R., Englander, W., and Degrado, W. F. (1996) *Proteins: Struct., Func., Gen. 24*, 427−432.
34. Pace, C. N., Laurents, D. V., and Thomson, J. A. (1990) *Biochemistry 29*, 2564−2572.
35. Richards, F. M., Wyckoff, H. W., Carlson, W. D., Allewell, N. M., Lee, B., and Mitsui, Y. (1971) *Cold Spring Harbor Symp. Quant. Biol. 36*, 34−43.
36. Myers, J. K., Pace, C. N., and Scholtz, J. M. (1995) *Protein Sci. 4*, 2138−2148.
37. Smith, J. S., and Scholtz, J. M. (1996) *Biochemistry 35*, 7292−7297.

BI972402Y